metals

Article

Laser-MIG Hybrid Welding–Brazing Characteristics of Ti/Al Butt Joints with Different Groove Shapes

Xin Zhao [1,*], Zhibin Yang [2], Yonghao Huang [2], Taixu Qu [1], Rui Cheng [1] and Haiting Lv [1]

[1] School of Mechanical Engineering, Dalian University of Science and Technology, Dalian 116052, China
[2] School of Materials Science and Engineering, Dalian Jiaotong University, Dalian 116028, China
* Correspondence: zhaoxin881@126.com; Tel.: +86-13942859690

Abstract: TC4 titanium alloy and 5083 aluminum alloy with different groove shapes were joined by laser-MIG hybrid welding–brazing using ER4043 filler wire. The effects of groove shape on the weld formation, intermetallic compounds and tensile property of the Ti/Al butt joints were investigated. The welds without obvious defects could be obtained with grooves of I-shape and V-shape on Ti side, while welds quality with grooves of V-shape on Al side and V-shape on both sides were slightly worse. The interfacial intermetallic compounds (IMCs) on the brazing interface were homogeneous in the joints with groove of V-shape on Ti side, and V-shape on both sides, which had similar thickness and were both composed of $TiAl_3$. Unlike the IMCs mainly composed of $TiAl_3$ at the I-shape groove interface, $TiAl_3$, TiAl, and Ti_3Al constituted the IMCs at the V-shape on Al side interface. The average tensile strength of Ti/Al joints with groove of I-shape was the highest at 238 MPa, and was lowest at 140 MPa with groove of V-shape on Al side. The tensile samples mainly fractured at IMCs interface and the fractured surfaces all exhibited mixed brittle–ductile fracture mode. Based on the above research results, I-shape groove was recommended for laser-arc hybrid welding–brazing of 4 mm thick Ti/Al dissimilar butt joints.

Keywords: Ti/Al dissimilar metal; laser-MIG hybrid welding–brazing; weld formation; intermetallic compounds; tensile property; groove shape

Academic Editor: Dariusz Rozumek

Received: 3 May 2025
Revised: 28 May 2025
Accepted: 30 May 2025
Published: 31 May 2025

Citation: Zhao, X.; Yang, Z.; Huang, Y.; Qu, T.; Cheng, R.; Lv, H. Laser-MIG Hybrid Welding–Brazing Characteristics of Ti/Al Butt Joints with Different Groove Shapes. *Metals* **2025**, *15*, 625. https://doi.org/10.3390/met15060625

1. Introduction

Due to low density, excellent mechanical properties, splendid corrosion resistance and outstanding high-temperature stability, titanium alloys have been widely applicated in aerospace, marine engineering, military equipment, and other high-end manufacturing fields [1]. But it is very unfortunate that the comparatively high cost of titanium alloys had limited their broader applications [2]. Compared with titanium alloys, aluminum alloys not only have the same advantages of high specific strength and good corrosion resistance, but also have lower application cost [3]. Therefore, Ti/Al composite structure combines the advantages of both titanium alloys and aluminum alloys, which has a favorable practical application prospect [4,5]. Welding has always been the main joining method for Ti/Al composite structures. However, Ti/Al dissimilar metals are rather difficult to weld together because of their extreme atrocious metallurgical compatibilities, which is also the root cause of its serious challenge in practical applications [6,7]. In particular, massive brittle intermetallic compounds (IMCs) would inevitably generate at the interface during the welding process [8], which would greatly deteriorate the mechanical properties of the dissimilar metal joints and make them unable to meet the requirements for practical

applications [9,10]. Therefore, how to obtain the high-quality welded joints of the dissimilar metals has always been a research focus for manufacturing Ti/Al composite structures.

Among the common welding methods, researchers almost unanimously recognize that the dissimilar metals welded by employing the conventional fusion welding method is nearly infeasible [11,12]. Brazing and pressure welding have been usually used for joining the dissimilar metals, but the low joint strength and special joint configuration extremely limit their application and promotion in the manufacturing field [6,13,14]. In recent years, the welding–brazing method has been proposed and gradually applied for joining the dissimilar metals. The alloy with low melting temperature was melted while the alloy with high melting temperature was still kept solid during the welding–brazing process, which could effectively suppress the growth of the IMCs growth at the interface and thereby significantly improve the tensile strength of the joints [15–17]. The traditional arc welding–brazing including tungsten inert gas welding–brazing (TIG) and metal inter gas welding–brazing (MIG) was firstly employed for joining the Ti/Al dissimilar metals [18], especially the MIG welding–brazing due to its low cost and superior gap tolerance [19]. However, the arc welding–brazing still faces the problem of relatively thick IMCs layer due to high heat input and low welding speed, which leads to a limited increase in the joint strength [20]. Considering the welded–brazed joint strength could be improved by reducing the thickness of the IMCs layer, laser welding–brazing is an efficient and reliable method due to its lower heat input and higher welding speed.

Recently, in order to achieve high-quality Ti/Al dissimilar joints, numerous studies have been carried out by using laser welding–brazing method. The research focus has always been on suppressing the IMCs formation and improving the joint performance, and the main research approach is welding–brazing process parameters optimization. Leo et al. [21] indicated that the thickness and shape of the IMCs layer of the Ti/Al laser welded–brazed joints obviously varied as the defocusing distance changed, the thinner and flatter IMCs layer could be obtained with negative defocusing distance due to the lower peak temperature at the interface, and which finally improved the tensile performance of the welded–brazed joints. Zhao et al. [22] demonstrated that the larger laser offset distance toward the aluminum alloy resulted in a lower degree of interfacial reactions during laser welding–brazing for Ti/Al dissimilar alloys, the average thickness of the IMCs layer decreased from about 15 μm to 5 μm when the laser offset distance increased from 0.3 mm to 0.7 mm, meanwhile the thinner IMCs thickness under larger laser offset distance lead to an obvious enhancement in the mechanical properties of the welded–brazed joints. But on the contrary, Malikov et al. [8] manifested that the laser offset toward titanium alloy rather than aluminum alloy during laser welding–brazing of Ti-Al-V and Al-Cu-Li dissimilar alloys could reduce the IMCs layer thickness, which could reduce from about 400 μm without laser offset to 2.5 μm and 0.7 μm, when the laser offset was 0.5 mm and 1.0 mm, the average tensile strength of the welded–brazed joints accordingly increased from 103 MPa to 213 MPa and 272 MPa. Xia et al. [23] found that the laser oscillated scanning path could reduce the thickness and improve homogeneity of the Ti/Al intermetallic compounds layer; adopting the circular scanning path would obtain the thinnest and most homogenous IMCs distribution duo to its lowest peak temperature and smallest peak temperature gradient. Additionally, Chen et al. [24] showed that the laser oscillation frequency had remarkable influences on the porosity defects and tensile strength of the Ti/Al welded–brazed joints. In order to more effectively control the IMCs layer thickness and improve the joints strength of the Ti/Al dissimilar joints, some unconventional laser welding–brazing methods have also been proposed. Zhang et al. [25] verified that the homogeneous thickness of IMCs layer could be obtained by using the dual laser bilateral synchronous welding–brazing method. Chen et al. [10] performed the experiments at a low vacuum condition and found

that the IMCs layer thickness could be controlled less than 2 μm due to the enhanced melt flow and uniform temperature field; meanwhile, the uniform IMCs distribution also could significantly improve the joint tensile strength.

However, the extremely strict assembly accuracy has been always required in laser welding process, which greatly limits its industrial application ranges. Laser-MIG hybrid welding combines the advantages of laser welding and arc welding including higher welding efficiency, smaller heat input, better process stability, and larger gap adaptability, which has been considered as an ideal method for improving weld quality. Therefor, laser-MIG hybrid welding–brazing has been successfully introduced to join the dissimilar metals. Casalino et al. [26] manifested that laser-MIG hybrid welding–brazing could contribute to bridge the gap and stabilize the weld pool, but the IMCs layer was quite irregular and inhomogeneous due to a large proportion of the heat input directly acting at the interface. Shaker et al. [27] pointed out that laser-MIG hybrid welding–brazing could limit the IMCs layer thickness and finally achieve better Fe/Al dissimilar joints, and emphasized that the exposure time to the heat source of the base metal during the welding–brazing process was very important for controlling the thickness of the IMCs layer. Gao et al. [28] indicated that the IMCs layer thickness was more sensitive to the laser power because the interface temperature was mainly depended on it during laser-MIG hybrid welding–brazing process, and found that the thickness and shape of the IMCs layer were both nonuniform along the interface from top to bottom. Xue et al. [29] showed that the IMCs layer thickness increased and its morphology transformed when the heat input promoted during the laser-MIG hybrid welding–brazing process of Fe/Al dissimilar metals, and the morphology transformed from compact layer to needle-like structure was beneficial for improving the joint tensile strength. Zhao et al. [30] clearly demonstrated that the energy ratio of laser and arc must be given priority consideration in the welding of dissimilar metals to reduce the microstructure inhomogeneity and achieve a desirable property balance among the hardness, toughness, and corrosion resistance. Wang et al. [31] obtained fine Ti/Al dissimilar butt joints by laser-MIG hybrid welding–brazing method, and showed that the IMCs layer had varying morphology and thickness in the different regions.

Selecting an appropriate groove shape is conducive to optimize process parameters and obtain high-quality joints, in addition, which also significantly influenced the IMCs formation and the joints performance [32,33]. In the present work, Ti/Al dissimilar butt joints with different groove shapes were performed by laser-MIG hybrid welding–brazing. The influences of groove shape on weld formation, intermetallic compounds, and tensile property of the welded–brazed joints were investigated. The core objective of this work was to confirm an optimal groove shape for laser-MIG hybrid welding–brazing of Ti/Al butt joints.

2. Materials and Methods

TC4 titanium alloy and 5083 aluminum alloy with thickness of 4.0 mm were selected as base metals in this work, whose dimensions were machined to 150 mm (length) × 100 mm (width) × 4 mm (height). Four typical grove shapes including I-shape, V-shape on Ti side, V-shape on Al side, and V-shape on both sides were prepared, whose schematic diagrams are provided in Figure 1. Before laser-MIG hybrid welding–brazing, the base metal surface near welding–brazing region was firstly preprocessed by mechanical grinding and then scrubbing with acetone to remove the oxide film and greasy dirt. Finally, the TC4 surface was coated by noncorrosive flux suspension (KAlF4 power dissolved in acetone) with an average thickness of approximately 0.1 mm to improve the spreadability and wettability of the molten metal on the base metal surface. ER4043 filler wire with a diameter of 1.2 mm was selected as filler mater, this is mainly because this filler wire can be beneficial for

achieving better weld formation and tensile properties. The main chemical compositions of the base metal and filler wire are given in Table 1.

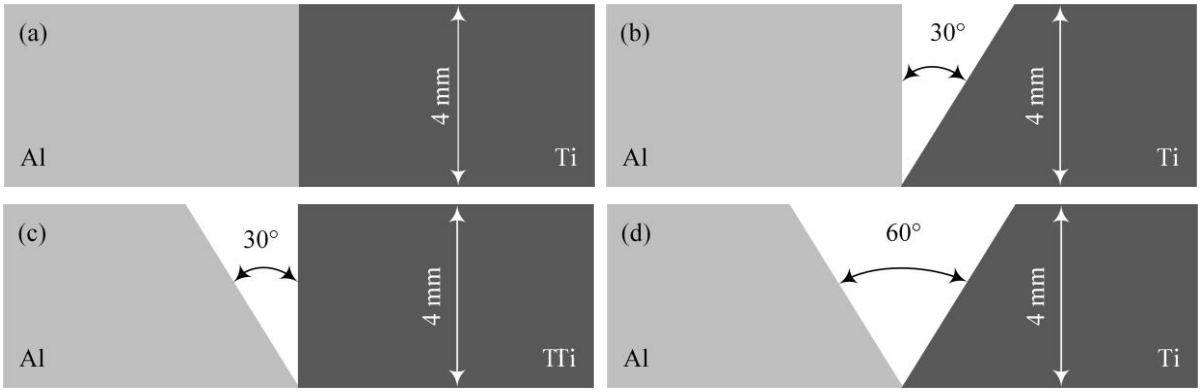

Figure 1. Schematic diagrams of groove shapes: (**a**) I-shape, (**b**) V-shape on Ti side, (**c**) V-shape on Al side, and (**d**) V-shape on both sides.

Table 1. Chemical compositions of base metal and filler wire (wt. %).

Metals	Al	Ti	Si	Fe	Cu	Mn	Zn	Mg	V
TC4	6.19	Bal.	/	0.21	/	/	/	/	3.95
5083	Bal.	0.12	0.34	0.37	0.08	0.65	0.19	4.57	/
ER4043	Bal.	0.18	5.27	0.61	0.26	0.04	0.11	0.05	/

The laser-MIG hybrid welding–brazing experiments were carried out by using a fiber laser (IPG YLS-6000, Burbach, Germany) in combination with a welding machine (Fronius TPS 500i CMT, Wels, Austria), which were synchronously and collaboratively controlled by a high precision six-axis welding robot (KUKA 30HA, Bavaria, Germany). The maximum output power of the laser was 6.0 kW. The laser beam was transmitted by a 100 μm core-diameter fiber, collimated by a lens with 150 mm focal length, and focused by a lens with 300 mm focal length. The emission wavelength and focus diameter of the laser were 1070 ± 5 nm and 0.2 mm, respectively. During the laser-MIG hybrid welding–brazing process, the distance between the laser beam and filler wire tip was about 3 mm, and the oblique angles between them and the base metals were 80° and 50°, respectively. The laser defocusing distance was about +2 mm. 99.999% high purity argon with a flow rate of 15 L/min was used as the shielding gas to protect the molten pool from pollution. The laser-MIG hybrid welding–brazing process adopted in this work ss shown in Figure 2. The samples were fixed on a plate with a groove (height 3 mm and width 6 mm); the purpose was to ensure that the back of the weld seam could be formed freely.

After laser-MIG hybrid welding–brazing experiments, the representative cross-section specimens taken from perpendicular to the welded–brazed joints, firstly mechanically ground with abrasive papers (#240, #400, #600, #800, #1000, and #1200), then polished with diamond polishing agents (2.5 μm and 1.0 μm), and finally etched with Keller's reagent (1 mL HF, 1.5 mL HCl, 2.5 mL HNO_3, and 95 mL H_2O) for about 15 s. The macroscopic features of the welded–brazed joints were observed by using an optical microscopy (OLYMPUS BX-51M, Tokyo, Japan). The microstructure of the IMCs and the fracture morphology of the tensile specimens were observed by using a scanning electron microscopy (SEM, ZEISS SUPRA 55, Jene, Germany). The chemical compositions of the IMCs layer were measured by using an energy dispersive spectrometer (EDS, ZEISS SUPRA 55, Jene, Germany). According to GB/T 228.1-2021 [34], the tensile tests were conducted by using an electronic universal testing machine (STAR WDW-300E, Jinan, China) with

a loading rate of 2 mm/min at room temperature. The tensile strength was taken from the average value of the two testing specimens. The tensile testing specimen retained the weld original reinforcement, and its geometric dimensions are shown in Figure 3. When calculating the tensile strength, the thickness of the joint is based on the actual thickness of the base metal.

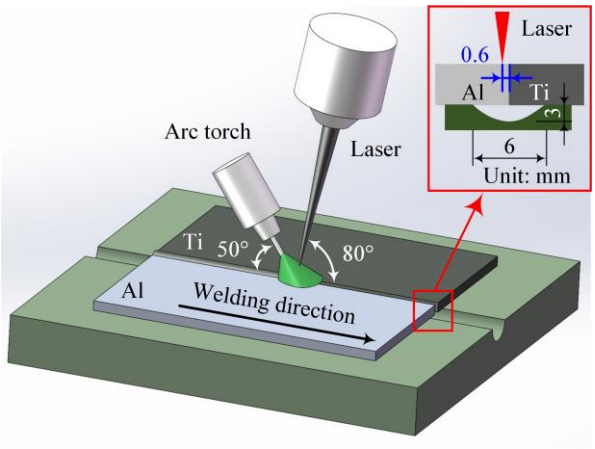

Figure 2. Schematic diagrams of laser-MIG hybrid welding–brazing process and laser offset distances.

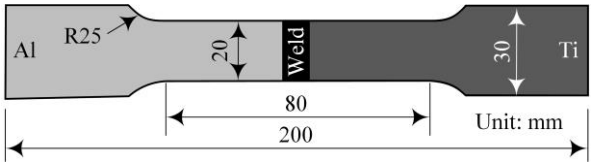

Figure 3. Schematic diagram of tensile testing specimen.

3. Results and Discussion

3.1. Weld Formation

Based on the quality of the weld formation, the optimized laser-MIG hybrid welding–brazing parameters for the four typical groove shapes were finally obtained after a large number of experiments, as listed in Table 2. It could find that except for the groove with V-shape on both sides which required double-pass welding due to the large groove should be filled, the other three groove types all could be welded by single-pass welding method. Compared with other groove shapes, the groove with I-shape required a higher laser power, but the welding current and welding voltage were relatively smaller. In addition, the welding speed of the groove with V-shape on Ti side was apparently lower than that of the other groove shapes.

Table 2. Laser-MIG hybrid welding–brazing parameters adopted for different groove types.

Groove Types	Welding Speed (m/min)	Laser Power (kW)	Wire Feeding Speed (m/min)	Welding Current (A)	Welding Voltage (V)	Laser Offset Distance (mm)	Notes
I-shape	1.5	2.2	6.5	112	18.2	0.6	/
V-shape on Ti side	0.8	1.8	8.0	180	21.7	0.2	/
V-shape on Al side	1.8	1.6	9.0	204	23.3	0.4	/
V-shape on both sides	1.8	1.5	7.5	126	18.8	0.6	Backing
	1.5	1.5	9.0	204	23.3	0.6	Covering

The laser offset distances and welds formation with the different groove shapes as shown in Figure 4. The results indicated that the laser offset distance should be towards aluminum alloy to achieve the effective joining of the Ti/Al dissimilar butt joints. The reasonable laser offset distances were, respectively, 0.6 mm, 0.2 mm, 0.4 mm, and 0.6 mm for the grooves with I-shape, V-shape on Ti side, V-shape on Al side, and V-shape on both sides, as shown in Figure 4a,d,g,j.

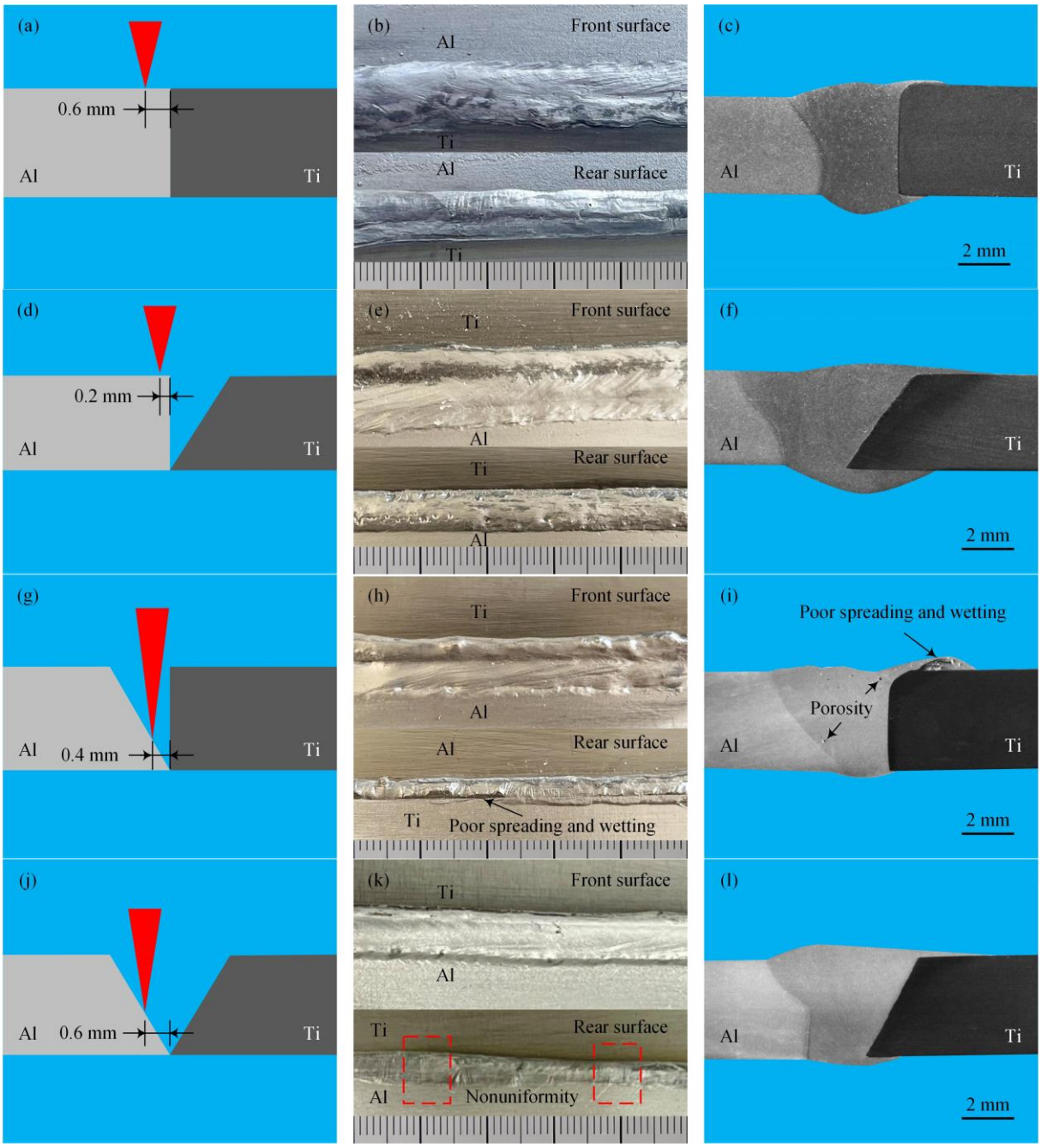

Figure 4. Laser offset distances and welds formation with different groove types: (**a**–**c**) I-shape; (**d**–**f**) V-shape on Ti side; (**g**–**i**) V-shape on Al side; (**j**–**l**) V-shape on both sides. Unit: mm.

From the perspective of the weld surface formation, it could find that the front surface and rear surface were all well-formed for the grooves with I-shape and V-shape on Ti side; there were no obvious defects that could be observed as shown in Figure 4b,e. The spreading and wetting of molten pool on the rear surface of the base metal became worse

for the grooves with V-shape on Al side and V-shape on both sides. Some regions were not effectively spread for the groove with V-shape on Al side as shown in Figure 4h, which would significantly deteriorate the tensile performance of the welded–brazed joints. The spreading and wetting of the whole length weld seam were nonuniformity for the groove with V-shape on both sides as shown in Figure 4k, which was also detrimental for obtaining welded–brazed joints with uniform tensile performance. Judging only from the experimental results of the weld surface forming quality with different groove shapes, it could be found that the groove with V-shape groove machined on the Al side was not conducive to obtain high-quality Ti/Al dissimilar joints, the main reason was that the molten pool spread and wet on the base metal rear surface was relatively poor.

From the perspective of the weld cross-section formation, the high-quality welds without obvious defects all could be obtained with the grooves with I-shape, V-shape on Ti side and V-shape on both sides, and the molten pool spread and wet well on the surface of the base metals, as shown in Figure 4c,f,l. The experimental results demonstrated that the titanium alloy almost had not melted during the laser-MIG hybrid welding–brazing process, and the spreadbility and wettability of the molten pool on the titanium alloy surface was related to the groove shape for the Ti side. However, unfortunately, a certain number of porosity defects were observed on the weld cross-section of the groove with V-shape on Al side as shown in Figure 4i. Compared with the other groove types, the poor spreading and wetting had only appeared on the front surface of the titanium alloy, which was probably because the apparent melting had occurred at the groove upper part of Ti side. Meanwhile, the spreading and wetting length of the molten pool on the rear surface of titanium alloy was extremely small, which indicated that there was almost no spread and wet formed on the rear surface for the Ti side.

3.2. Intermetallic Compounds

The morphology, phase, and thickness of the IMCs layer had crucial influence on the tensile strength of the welded–brazed dissimilar metal joints [35]. In the present study, three regions including top, middle, and bottom, along the brazing interface, were selected to deep analysis the influences of the groove shapes on the IMCs layer. The IMCs layer microstructures of the laser-MIG hybrid welded–brazed Ti/Al butt joints with different groove shapes as shown in Figure 5. Furthermore, the EDS composition analysis was carried out at the locations which marked as 1–16 in Figure 5, and the results were given in Table 3.

For the joint with groove of I-shape, a two-layer IMCs in the top region had consisted of 1.4 μm thick continuous serrate-shaped IMCs near the Ti base metal and noncontinuous rod-like IMCs near the fusion zone, as shown in Figure 5a. According to Table 3, the Ti/Al atomic rations in locations 1 and 2 were both about 1:3, thus, it could be inferred that the serrate-shaped and rod-like IMCs would both probably be $TiAl_3$. $TiAl_3$ was also written as $Ti(Al,Si)_3$ in some relevant research papers because Al and Si atoms have similar crystal structures [36,37]. Meanwhile, it could be found that some rod-like $TiAl_3$ were broken in the weld, which was mostly due to the vigorous stirring of the molten pool caused by the higher laser power. The difference was that only continuous serrate-shaped IMCs layer could be observed both in the middle and bottom regions, as shown in Figure 5b,c. Their thickness was 1.6 μm and 1.0 μm, and the EDS analysis results indicated the IMCs also could be $TiAl_3$. Meanwhile, it could also be found that there was no defect that appeared near the IMCs layer in all regions.

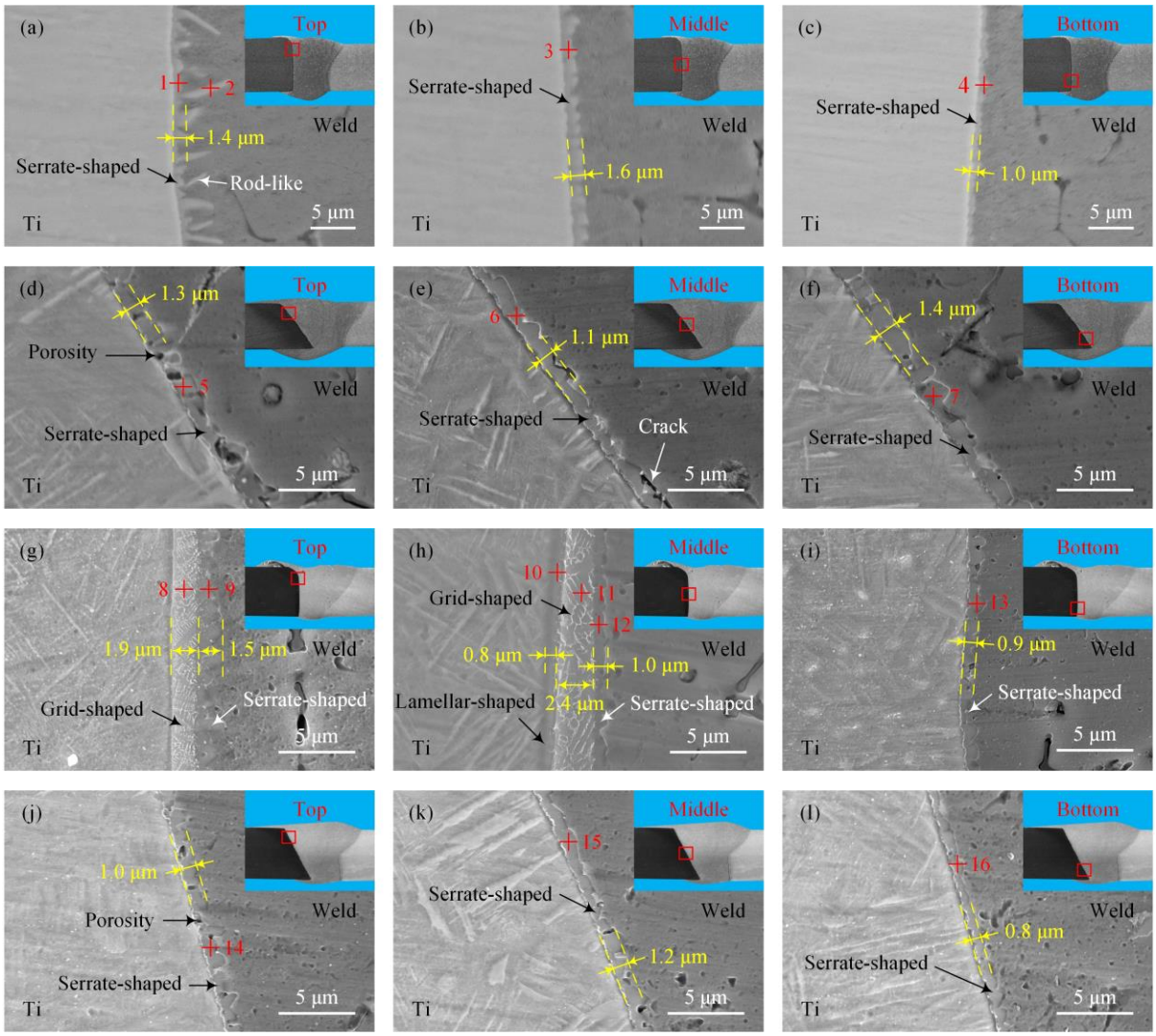

Figure 5. Interfacial intermetallic compounds (IMCs) microstructures with different groove types: (**a**–**c**) I-shape; (**d**–**f**) V-shape on Ti side; (**g**–**i**) V-shape on Al side; (**j**–**l**) V-shape on both sides.

Table 3. EDS composition analysis results of locations 1–16 in Figure 5 (at. %).

Locations	Al	Ti	Si	Possible Phase
1	72.31	23.23	4.46	$TiAl_3$
2	71.62	24.73	3.65	$TiAl_3$
3	69.56	24.32	6.12	$TiAl_3$
4	77.24	21.21	1.55	$TiAl_3$
5	73.21	23.07	3.72	$TiAl_3$
6	75.34	23.91	0.75	$TiAl_3$
7	71.23	22.43	6.34	$TiAl_3$
8	56.32	42.21	1.47	TiAl
9	72.34	23.42	4.24	$TiAl_3$
10	28.89	67.91	3.2	Ti_3Al
11	47.21	50.34	2.45	TiAl
12	71.54	22.45	6.01	$TiAl_3$
13	70.23	25.96	3.81	$TiAl_3$
14	77.33	21.24	1.43	$TiAl_3$
15	73.52	23.75	4.73	$TiAl_3$
16	74.27	24.46	1.27	$TiAl_3$

For the joints with groove of V-shape on Ti side and V-shape on both sides, the IMCs layer in the top, middle, and bottom regions were all only composed of continuous serrate-shaped IMCs, as shown in Figure 4d–f,j–l. The EDS composition analysis results of locations 5–7 and 14–16 in Table 3 indicated that the chemical compositions of the above IMCs were all almost the same with that of $TiAl_3$. Meanwhile, the thickness of the IMCs layers in the different regions did not have a very prominent difference. The results indicated that the IMCs layers of the grooves with V-shape on Ti side and V-shape on both sides were almost the same. However, it was worth noting that some porosity defects could be observed in the IMCs layer for the two above groove shapes, as shown in Figure 5d,f,j,k. More seriously, the crack occurred at the interface between the IMCs layer and the fusion zone as shown in Figure 5e. The porosity and crack defects would further reduce the tensile strength of the welded–brazed joints [38].

For the joint with groove of V-shape on Al side, there was a two-layer IMCs layer observed in the top regions, which was composed of 1.9 μm thick grid-shaped IMCs near the Ti base metal and 1.5 μm thick serrate-shaped IMCs near the fusion zone, as shown in Figure 5g. However, the IMCs transformed into a more complex three-layer structure: 0.8 μm thick lamellar-shaped IMCs near the Ti base metal, 1.0 μm thick serrate-shaped IMCs near the fusion zone, and 2.4 μm thick grid-shaped IMCs between them, as shown in Figure 5h. The IMCs layer in the bottom region was the only continuous serrate-shaped IMCs with a thickness of 0.9 μm as shown in Figure 5i, but a few porosity defects were found between the IMCs layer and the fusion zone. According to the EDS composition analysis results in Table 3, the grid-shaped and lamellar-shaped IMCs could be, respectively, determined as TiAl and Ti_3Al; the serrate-shaped IMCs still might be $TiAl_3$. The reason for the transformation in the morphology and composition of the IMCs layer was probably that Ti base metal was subjected to more arc action and excessive heat input [39].

3.3. Tensile Property

The tensile testing results of the laser-MIG hybrid welded–brazed Ti/Al butt joints with different groove shapes as shown in Figure 6. It could be found that the groove shape had obvious influence on the tensile properties of the welded–brazed Ti/Al butt joints. The average tensile strength of the welded–brazed joints with different groove shapes from high to low was as follows: I-shape, V-shape on Ti side, V-shape on both sides, and V-shape on Al side; meanwhile, the elongation also had the same change rule, as shown in Figure 6b. Compared with the joints of other groove shapes, the lowest tensile strength was obtained when the groove with V-shape on the Al side mainly due to its thickest IMCs layer generated at the interface. This corresponding relation indicated that the thick IMCs layer would reduce the tensile strength of the welded–brazed joints. In addition, the extremely small spreading and wetting distance of the molten pool on the Ti base metal rear surface further deteriorated the tensile performance of the welded–brazed joints [31]. Compared with joints of I-shape groove, the porosity and even crack defects existing in the IMCs layer of the joints with grooves of V-shape on Ti side and V-shape on both sides were the main reason for the reduction of the tensile strength. The fracture of the tensile testing specimens all initiated at the IMCs layer, the crack propagated along the interface for the joints with grooves of I-shape, V-shape on Ti side, and V-shape on Al side, but the crack propagated in the fusion zone for the joints with grooves of V-shape on both sides, as shown in Figure 6b.

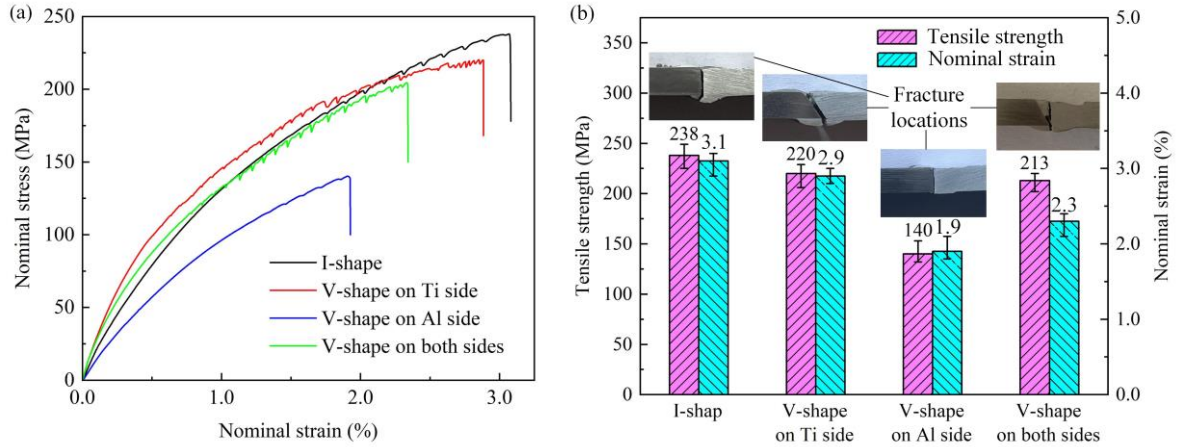

Figure 6. Tensile testing results of Ti/Al joints with different groove shapes: (**a**) stress–strain curves, and (**b**) tensile properties.

The fracture features of the tensile testing specimens of the joints with different groove shapes as shown in Figure 7. The EDS composition analysis results in different locations is given in Table 4. From the macrographs of the fracture surface, it could be found that there were some flat areas of different scales existing for the four typical groove shapes, as shown in Figure 7a,d,g,j. According to the EDS analysis results of locations 1, 2, 3 and 4, in Figure 7b,e,h,k, it could be suggested that the flat area was Ti base metal rather than IMCs. However, some IMCs of $TiAl_3$ might exist in location 5. The results also indicated that the facture crack first initiated between the Ti base metal and the IMCs layer, and showed typical brittle fracture mode. The EDS analysis result of location 6 in Figure 7c indicated that this area was mainly composed of Al atoms, which indicated that the weld metal showed a typical ductile fracture mode due to some dimples observed there, as shown in Figure 7c,f,i,l. By comparison, it could also find that the tensile strength of the welded–brazed joints was related to the area size of the flat scale, and the smaller area size had the higher tensile strength. This corresponding relation also indicated that the metallurgical bonding area size at the interface was an important factor affecting the tensile strength of the Ti/Al welded–brazed butt joints.

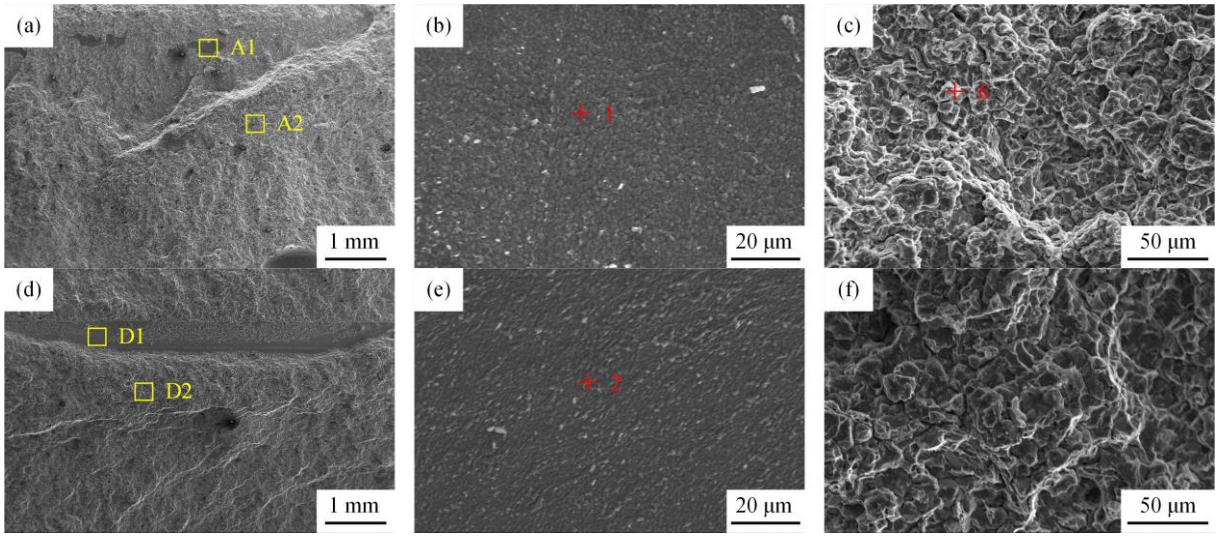

Figure 7. *Cont.*

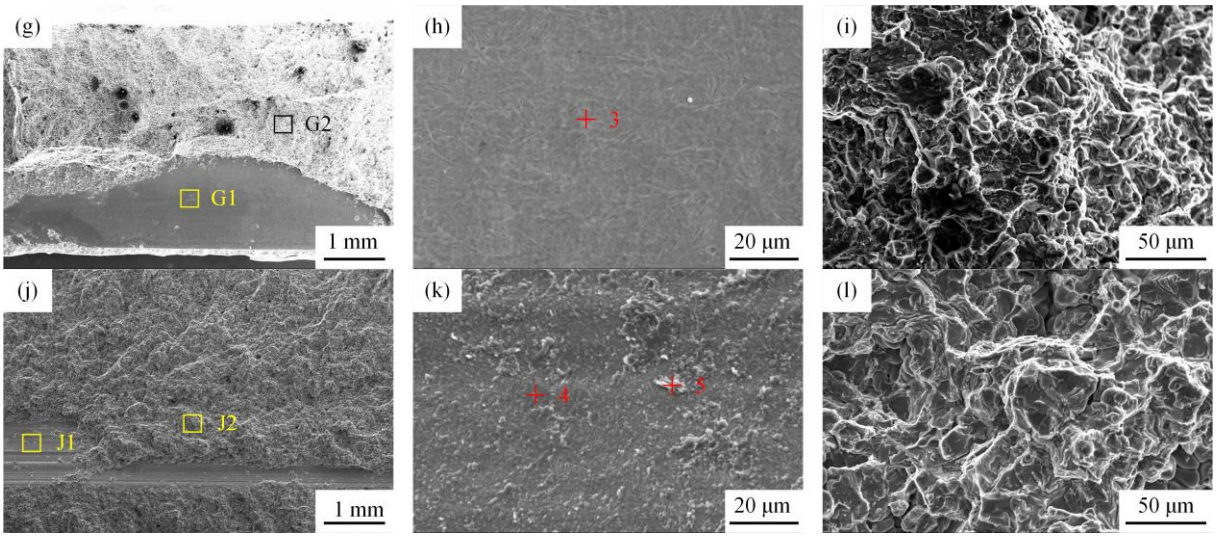

Figure 7. Fracture features of the joints with different groove types: (**a**) macrograph with I-shape, (**b**) details of area A1, (**c**) details of area A2, (**d**) macrograph with V-shape on Ti side, (**e**) details of area D1, (**f**) details of area D2, (**g**) macrograph with V-shape on Al side, (**h**) details of area G1, (**i**) details of area G2, (**j**) macrograph with V-shape on both sides, (**k**) details of area J1, and (**l**) details of area J2.

Table 4. EDS composition analysis results of locations 1–6 in Figure 7 (at. %).

Locations	Ti	Si	Al
1	90.37	3.76	5.87
2	91.26	3.15	5.59
3	90.85	3.02	6.13
4	90.19	3.05	6.76
5	23.18	2.55	74.29
6	0.17	5.76	94.57

4. Conclusions

For the grooves with I-shape, V-shape on Ti side, and V-shape on both sides, the high-quality welds without obvious defects could be obtained. The spreading and wetting were nonuniformity along the whole weld for the groove with V-shape on both sides. The groove with V-shape groove machined on the Al side was not conducive to obtain high-quality Ti/Al dissimilar butt joints.

For the joint with I-shape groove, two-layer IMCs composed of serrate-shaped and rod-like IMCs observed in the top region, and only serrate-shaped IMCs layer observed in the middle and bottom regions, the phase composition of the IMCs were all $TiAl_3$.

For the joints with groove of V-shape on Ti side and V-shape on both sides, the IMCs in the top, middle, and bottom regions were all composed of serrate-shaped IMCs with similar thickness; and the phase compositions of the IMCs were all $TiAl_3$.

For the joint with groove of V-shape on Al side, the IMCs layer was obviously inhomogeneous: two-layer, three-layer, and single-layer IMCs were observed in the top, middle, and bottom regions along the interface. The phase compositions of the IMCs include lamellar-shaped TiAl, grid-shaped Ti_3Al, and serrate-shaped $TiAl_3$.

For the Ti/Al welded–brazed butt joints with different groove shapes, the average tensile strength from high to low was as follows: I-shape, V-shape on Ti side, V-shape on both sides, and V-shape on Al side. The fractured surfaces exhibited mixed brittle–ductile fracture mode, and the metallurgical bonding area size at the interface was an important factor affecting the tensile strength of them.

Based on the above research results, I-shape groove was recommended for laser-arc hybrid welding–brazing of 4 mm thick Ti/Al dissimilar butt joints.

Author Contributions: Conceptualization, X.Z. and Z.Y.; methodology, X.Z. and Z.Y.; validation, X.Z., Z.Y. and Y.H.; formal analysis, Y.H., T.Q. and R.C.; investigation, Y.H. and H.L.; resources, Z.Y.; data curation, Y.H. and Z.Y.; writing—original draft, Z.Y.; writing—review and editing, X.Z. and Z.Y.; visualization, T.Q. and R.C.; supervision, X.Z. and Z.Y.; project administration, Z.Y.; funding acquisition, X.Z. All authors have read and agreed to the published version of the manuscript.

Funding: This research was funded by Self-developed Research Project of Dalian University of Science and Technology, grant number KY24L003-ZL.

Data Availability Statement: The original contributions presented in this study are included in the article. Further inquiries can be directed to the corresponding author.

Conflicts of Interest: The authors declare no conflicts of interest.

References

1. Xin, S.; Liu, X.; Zhang, S.; Zhou, W.; Li, Q.; Guo, D.; Guo, P.; Zhang, P. An overview on research and development of low-cost titanium alloys. *Rare Met. Mat. Eng.* **2023**, *52*, 3971–3980.
2. Williams, J.C.; Boyer, R.R. Opportunities and issues in the application of titanium alloys for aerospace components. *Metals* **2020**, *10*, 705. [CrossRef]
3. Liu, S.S.; Yue, X.; Li, Q.Y.; Peng, H.L.; Dong, B.X.; Liu, T.S.; Yang, H.Y.; Fan, J.; Shu, H.L.; Qiu, F.; et al. Development and applications of aluminum alloys for aerospace industry. *J. Mater. Res. Technol.* **2023**, *27*, 944–983. [CrossRef]
4. Soni, R.; Verna, R.; Gary, R.K.; Sharma, V. A critical review of recent advances in the aerospace materials. *Mater. Today Proc.* **2024**, *113*, 180–184. [CrossRef]
5. Möller, F.; Thomy, C.; Vollertsen, F. Joining of titanium aluminum seat tracks for aircraft applications system technology and joint properties. *Weld. World* **2012**, *56*, 108–114. [CrossRef]
6. Zhao, H.; Yu, M.; Jiang, Z.; Zhou, L.; Song, X. Interfacial microstructure and mechanical properties of Al/Ti dissimilar joints fabricated via friction stir welding. *J. Alloys Compd.* **2019**, *789*, 139–149. [CrossRef]
7. Quazia, M.M.; Ishaka, M.; Fazalb, M.A.; Arslanc, A.; Rubaieeb, S.; Qabane, A.; Aimana, M.H.; Sultanf, T.; Alig, M.M.; Manladanh, S.M. Current research and development status of dissimilar materials laser welding of titanium and its alloys. *Opt. Laser Technol.* **2020**, *126*, 106090. [CrossRef]
8. Malikov, A.; Vitoshkin, I.; Orishich, A.; Filippov, A.; Karpov, E. Microstructure and mechanical properties of laser welded joints of Al-Cu-Li and Ti-Al-V alloys. *J. Manuf. Process.* **2020**, *53*, 201–212. [CrossRef]
9. Chen, S.; Li, L.; Chen, Y.; Huang, J. Joining mechanism of Ti/Al dissimilar alloys during laser welding-brazing process. *J. Alloy. Compd.* **2011**, *509*, 891–898. [CrossRef]
10. Chen, X.; Lei, Z.; Chen, Y.; Han, Y.; Jiang, M.; Tian, Z.; Bi, J.; Lin, S. Microstructure and tensile properties of Ti/Al dissimilar joint by laser welding-brazing at sub-atmospheric pressure. *J. Manuf. Process.* **2020**, *56*, 19–27. [CrossRef]
11. Guo, S.; Peng, Y.; Cui, C.; Gao, Q.; Zhu, J. Microstructure and mechanical characteristics of re-melted Ti-6Al-4V and Al-Mg-Si alloys but weld. *Vacuum* **2018**, *154*, 58–67. [CrossRef]
12. Nandagopal, K.; Kailasanathan, C. Analysis of mechanical properties and optimization of gas tungsten arc welding (GTAW) parameters on dissimilar metal titanium (6Al-4V) and aluminum 70575 by Taguchi and ANOVA techniques. *J. Alloy Compd.* **2016**, *682*, 503–516. [CrossRef]
13. Xia, Y.; Ma, Z.; Du, Q.; Jiu, Y.; Guo, P.; Qin, J.; Li, S.; Zhang, X.; Zhou, P.; Hu, J.; et al. Microstructure and properties of the TiAl/GH3030 dissimilar joints vacuum-brazed with a Ti-based amorphous filler metal. *Mater. Charact.* **2024**, *207*, 113520. [CrossRef]
14. Chang, S.Y.; Tsao, L.C.; Lei, Y.H.; Mao, S.M.; Huang, C.H. Brazing of 6061 aluminum alloy/Ti-6Al-4V using Al-Si-Cu-Ge filler metals. *J. Mater. Process. Tech.* **2012**, *212*, 8–14. [CrossRef]
15. Gao, M.; Chen, C.; Gu, Y.; Zeng, X. Microstructure and tensile behavior of laser arc hybrid welded dissimilar Al and Ti alloys. *Materials* **2014**, *7*, 1590–1602. [CrossRef]
16. Adamiak, M.; Wyględacz, B.; Czupryński, A.; Górka, J. A study of susceptibility and evaluation of causes of cracks formation in braze-weld filler metal in lap joints aluminum—Carbon steel made with use of CMT method and high-power diode laser. *Arch. Metall. Mater.* **2017**, *62*, 2113–2123. [CrossRef]
17. Li, Z.; Zhang, Y.; Yang, Y.; Feng, J.; Zhang, L. Properties study on Ti/Al butt joining by GMAW/GTAW hybrid welding-brazing. *Mater. Res. Express* **2023**, *10*, 116518. [CrossRef]

18. Zhou, X.; Zhao, H.; Liu, F.; Yang, B.; Chen, B.; Tan, C. Influence of energy ration on microstructure and mechanical properties in the transition zone of hybrid laser-MIG welded Ah36/316L dissimilar joints. *J. Mater. Res. Technol.* **2021**, *15*, 4487–4501. [CrossRef]
19. Song, L.; Wei, S.; Rao, W.; Li, Z.; Zhang, Y. Optimization of welding parameters during Ti-TA2/5A06Al dissimilar double-sided cold arc metal inert gas welding. *J. Mater. Eng. Perform.* **2022**, *31*, 9714–9726. [CrossRef]
20. Xu, W.; Wang, W.; Yang, Q.; Xiong, J.; Zhang, L.; He, H. CMT twin welding-brazing of aluminum to titanium. *Weld. World* **2022**, *66*, 1121–1130. [CrossRef]
21. Leo, P.; D'Ostuni, S.; Nobile, R.; Mele, C.; Tarantino, A.; Casalino, G. Analysis of the process parameters, post-weld heat treatment and peening effects on microstructure and mechanical performance of Ti-Al dissimilar laser weldings. *Metals* **2021**, *11*, 1257. [CrossRef]
22. Zhao, J.; Geng, S.; Jiang, P.; Song, M.; Xu, B.; Luo, Q. Experimental and numerical research on formation mechanism of intermetallic compounds in laser brazing welding for Ti/Al dissimilar alloy. *J. Mater. Res. Technol.* **2024**, *31*, 2930–2944. [CrossRef]
23. Xia, H.; Zhang, S.; Wu, J.; Ma, Y.; Xu, L.; Li, H.; Yuan, J.; Yang, B.; Tan, C.; Wu, T. Homogenizing interfacial IMC distribution and enhancing strength of laser welded-brazed Al/Ti butt joint by oscillated scanning. *J. Mater. Res. Technol.* **2025**, *35*, 6226–6236. [CrossRef]
24. Chen, X.; Lei, Z.; Chen, Y.; Han, Y.; Jiang, M.; Tian, Z.; Bi, J.; Lin, S.; Jiang, N. Effect of laser beam oscillation on laser welding-brazing of Ti/Al dissimilar metals. *Materials* **2019**, *12*, 4165. [CrossRef]
25. Zhang, J.; Zhao, J.; Hu, K.; Gao, Q.; Zhan, X. Improving intermetallic compounds inhomogeneity of Ti/Al butt joints by dual laser-beam bilateral synchronous welding-brazing. *Opt. Laser Technol.* **2022**, *146*, 107533. [CrossRef]
26. Casalino, G.; Leo, P.; Mortello, M.; Perulli, P.; Varone, A. Effects of laser offset and hybrid welding on microstructure and IMC in Fe-Al dissimilar welding. *Metals* **2017**, *7*, 282. [CrossRef]
27. Shaker, M.A.; Jain, M.K.; Chen, J.Z. Deformation behavior of steel-to-aluminum tailor blanks made by laser/MIG hybrid and cold metal transfer brazing methods. *Int. J. Adv. Manuf. Technol.* **2020**, *110*, 3061–3076. [CrossRef]
28. Gao, M.; Chen, C.; Mei, S.; Wang, L.; Zeng, X. Parameter optimization and mechanism of laser-arc hybrid welding of dissimilar Al alloy and stainless steel. *Int. J. Adv. Manuf. Technol.* **2014**, *74*, 199–208. [CrossRef]
29. Xue, J.; Li, Y.; Chen, H.; Zhu, Z. Effects of heat input on wettability, interface microstructure and properties of Al/steel butt joint in laser-metal inert-gas hybrid welding-brazing. *J. Mater. Process. Tech.* **2018**, *255*, 47–54. [CrossRef]
30. Zhao, Y.; Sun, H.; Zhao, X.; Zhao, H.; Liu, F.; Yang, B.; Chen, B.; Tan, C. The effect of inhomogeneous microstructure on the properties of laser-MIG hybrid welded 316L/AH36 dissimilar joints. *J. Mater. Res. Technol.* **2024**, *28*, 4088–4096. [CrossRef]
31. Wang, W.; Zhu, Z.; Xue, J. Microstructure and mechanical properties of Ti/Al dissimilar joints produced by laser-MIG welding-brazing. *Int. J. Mod. Phys. B* **2019**, *33*, 1940030. [CrossRef]
32. Tomashchuk, I.; Sallamand, P.; Méasson, A.; Cicala, E.; Duband, M.; Peyre, P. Aluminum to titanium laser welding-brazing in V-shaped groove. *J. Mater. Process. Technol.* **2017**, *245*, 24–36. [CrossRef]
33. Li, P.; Lei, Z.; Zhang, X.; Cai, E.; Chen, Y. The microstructure and mechanical properties of dual-spot laser welded-brazed Ti/Al butt joints with different groove shapes. *Materials* **2020**, *13*, 5105. [CrossRef]
34. *GB/T 228.1-2021*; Metallic Materials—Tensile Testing—Part 1: Method of Test at Room Temperature. Standards Press of China: Beijing, China, 2021.
35. Kuryntsev, S. A review: Laser welding of dissimilar materials (Al/Fe, Al/Ti, Al/Cu)-methods and techniques, microstructure and properties. *Materials* **2022**, *15*, 122. [CrossRef] [PubMed]
36. Chen, S.; Li, L.; Chen, Y. Interfacial reaction mode and its influence on tensile strength in laser joining Al alloy to Ti alloy. *Mater. Sci. Technol.* **2010**, *26*, 230–235. [CrossRef]
37. Chen, Z.; Cai, C.; Yu, J.; Huang, J.; Chen, H.; Li, L. Microstructure evolution and fracture behavior of laser welded-brazed titanium/aluminum joints with various gap sizes. *J. Mater. Res. Technol.* **2024**, *29*, 714–727. [CrossRef]
38. Chen, L.; Wang, C.; Xiong, L.; Zhang, X.; Mi, G. Microstructural, porosity and mechanical properties of lap joint laser welding for 5182 and 6061 dissimilar aluminum alloys under different place configurations. *Mater. Des.* **2020**, *191*, 108625. [CrossRef]
39. Wei, S.; Li, Y.; Wang, J.; Liu, K. Influence of welding heat input on microstructure of Ti/Al joint during pulsed gas metal arc welding. *Mater. Manuf. Process.* **2014**, *29*, 954–960. [CrossRef]